THE ORIGIN OF FORBIDDEN SPECTRA IN ELECTRON PARAMAGNETIC RESONANCE

V. N. LAZUKIN, A. N. TERENT'EVSKIĬ, and B. V. OZHEREL'EV

Institute of Nuclear Physics, Moscow State University

Submitted May 8, 1968

Zh. Eksp. Teor. Fiz. 55, 1612–1618 (November, 1968)

The spectrum of forbidden EPR transitions is considered for Mn^{2+} ions in a calcite lattice, with and without inclusion of the hyperfine structure. It is shown that the ordinary spin Hamiltonian formalism provides a fully satisfactory description of experimental observations. The effect of the crystal field on the positions of the EPR spectra with selection rules $\Delta M = R$ and $\Delta m_I = r$ is determined. The pattern of forbidden lines in a field H depends on the fine-structure splitting of Zeeman levels by the crystal field. Quadrupole interactions, to which some authors[4] attribute the presence of a spectrum that is nuclear-spin forbidden, could not be detected. Finally, it is affirmed that the forbidden electronic and nuclear transitions have an identical origin.

In addition to the lines that are allowed by the ordinary selection rules the spectra of atoms and molecules are known to include weak lines representing transitions that are associated with different selection rules. These "forbidden" lines are observed both in the optical and in lower frequency regions. Several investigators have observed a forbidden electron paramagnetic resonance (EPR) spectrum of certain ions in crystals.[1-8] Although the origin of forbidden optical spectra is clearly determinable, as a general rule, the same cannot be said regarding the forbidden EPR spectra.

The present work is concerned with experimental observation of the forbidden EPR spectrum of Mn^{2+} ions in an axially symmetric crystal system ($CaCO_3$).

1. FINE-STRUCTURE SPLITTING

The ground state of Mn^{2+} is known to be a singlet having sixfold spin degeneracy (^6S). This degeneracy is removed partially by the crystal field, to an extent that depends on the symmetry possessed by the latter. In a cubic field the singlet splits into twofold and fourfold degenerate spin levels,[9-11] while in fields possessing a lower order of symmetry the degeneracy may be reduced to Kramers doublets.[12-14]

A suitable spin Hamiltonian for the case of axial symmetry can be written as[15]

$$\hat{H} = g_{\parallel}\beta H_z\hat{S}_z + g_{\perp}\beta(H_x\hat{S}_x + H_y\hat{S}_y) + B_2^0\hat{O}_2^0 + B_4^0\hat{O}_4^0 + B_4^3\hat{O}_4^3, \quad (1)$$

where the conventional notation has been used. In deriving our final equation we omit the term $B_4^3O_4^3$ because of its smallness. By means of familiar transformations, limiting ourselves to second-order perturbation theory corrections and assuming the selection rule $\Delta M = R$ ($R = 1, 2, 3, \ldots$) for the quantum number M, we finally obtain an expression that can be applied to the experimental results:

$$\begin{aligned} HR = {} & H_0 - {}^1/_2 DR(2M - R)(3\cos^2\theta - 1) \\ & + (D^2R/8H_0)[4S(S+1) - 24M(M-R) - (8R^2+1)]\sin^2 2\theta \\ & - (D^2R/8H_0)[2S(S+1) - 6M(M-R) - (2R^2+1)]\sin^4\theta, \end{aligned} \quad (2)$$

where H (the external field) and the constant terms H_0 and D are given in oersteds.

Transitions obeying the selection rule $\Delta M = 1$ are considered allowed, while transitions with $\Delta M = R \neq 1$ will be considered forbidden. For $\Delta M = R = 1$ our Eq. (2) becomes the well-known expression that describes the fine-structure splitting of spin levels in a crystal field.

Since Mn^{2+} has electron spin $S = {}^5/_2$ we can expect that the EPR spectrum of Mn^{2+} will include four forbidden fine-structure lines with $\Delta M = 2$, three forbidden lines with $\Delta M = 3$, two forbidden lines with $\Delta M = 4$, and one forbidden line with $\Delta M = 5$. After we locate experimentally the $\Delta M = 1$ fine-structure lines in a field H for zero angle θ between the applied magnetic field and the principal axis of the crystal, we can construct the behavior pattern of the spin levels in the field H.

The bottom of Fig. 1 shows where the allowed and forbidden lines are located in a field H; the upper part shows how the spin levels behave as the magnetic field is increased. Equation (2) provides an excellent de-

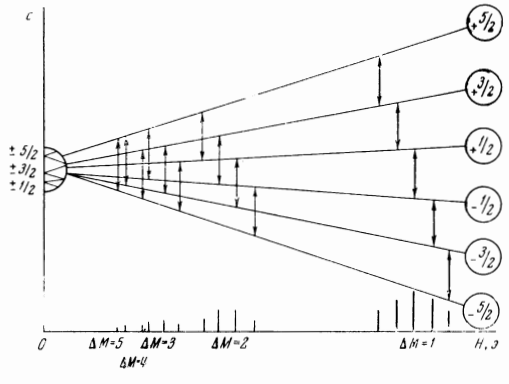

FIG. 1. Fine-structure transtions in a field H. The bottom line show five groups of lines: five lines obeying the selection rule $\Delta M = 1$ (allowed spectrum); four lines for $\Delta M = 2$. three lines for $\Delta M = 3$; two lines for $\Delta M = 4$, and one line for $\Delta M = 5$. The last four groups comprise the forbidden spectrum. The upper part of the figure shows the character of spin level splitting by the field H. The arrows correspond to the magnitude of the quanta $h\nu$. The semicircle shows (enlarged) the splitting of the fine-structure levels by the crystal field. Numerical experimental data are given in all our figures only for the $CaCO_3$ crystal. However the results can easily be extended to the EPR spectrum of any iron-group ion in an axially symmetric crystal system.

scription of this extrapolation for Mn^{2+} in $CaCO_3$ when we use the following values of the constants: H_0 = 3325 Oe and D = 93.7 Oe. The good agreement between theory and experiment shows the reasonableness of the extrapolation, which has also made it possible to determine the spin level splittings induced by the crystal field.

It was found that the lowest level is a $\pm\frac{1}{2}$ Kramers doublet (Fig. 1), separated by 10.8×10^{-2} cm^{-1} from a higher $\pm\frac{3}{2}$ level, which in turn is separated by 3.24×10^{-2} cm^{-1} from a still higher $\pm\frac{5}{2}$ level. It should be noted that this splitting was determined for the case in which the principal crystal axis was along the magnetic field ($\theta = 0$, corresponding to $g = g_{\parallel}$).

In addition to the EPR measurements for $g = g_{\parallel}$ ($\theta = 0$) we investigated the angular dependence of the Mn^{2+} fine-structure lines in $CaCO_3$. Figure 2 shows theoretical curves calculated with Eq. (2) for the fine-structure transitions $\frac{5}{2} \rightarrow \frac{3}{2}$ and $-\frac{3}{2} \rightarrow -\frac{5}{2}$. Each of these lines undergoes hyperfine splitting into six components. The hyperfine-structure transitions undergo identical shifts in the field H as the angle θ is varied from 0 to 90°. Our experimental results are represented by the small circles in Fig. 2. We note that the theoretical curves took account of the term $B_4^0 O_4^0$ in Eq. (1); this small and awkward term was excluded from (2). In most instances this term corrects the lines in the field H by at most 10 Oe, which represents no essential alteration of the forbidden transitions ($\Delta M = R \neq 1$).

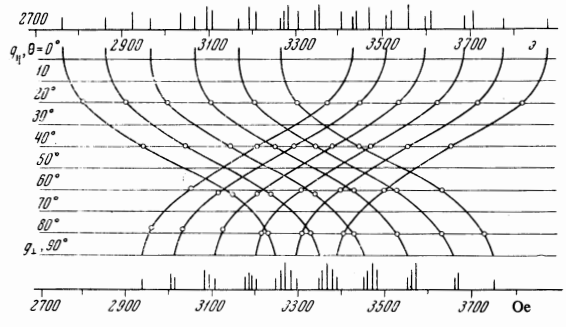

FIG. 2. Angular dependence of the fine-structure transitions 5/2 → 3/2 and −3/2 → −5/2 (each of which undergoes a hyperfine splitting into six components). The theoretical curves were calculated using Eq. (2) including the B_4^0 O_4^0 term; the small circles represent the experimental points. The separations of the hyperfine lines do not change as the angle θ varies from 0 to 90°.

Completely similar behavior of the fine-structure transitions $\frac{3}{2} \rightarrow \frac{1}{2}$ and $-\frac{1}{2} \rightarrow -\frac{3}{2}$ is observed for θ increasing from 0 to 90°. The only difference lies in the fact that the range of H within which the lines are shifted with varying θ is smaller than the range of H shown in Fig. 2. It should be noted that the described type of angle-dependent line shifts is characteristic of of all axial systems.

2. HYPERFINE SPLITTING

Despite numerous investigations[4,5,7,16] of the forbidden hyperfine spectrum, no satisfactory solution of the problem exists. This spectrum is either attributed incorrectly to a quadrupole interaction, or its observation is simply recorded without explanation. There has been no discussion of the relation between the forbidden spectrum in a field H and the character of spin-level splitting induced by the crystal field.

The hyperfine interaction is in the general case of dual character, consisting of a magnetic (dipole-dipole) interaction and an electric (quadrupole) interaction. Thus the spin Hamiltonian that takes account of the hyperfine interaction is represented by

$$\hat{H}_{hf} = \hat{A}\hat{S}\hat{I} + Q[\hat{I}_z^2 - \tfrac{1}{3}I(I+1)], \tag{3}$$

where A is the hyperfine structure constant, Q is the quadrupole interaction constant, and I is the nuclear spin.

We shall find the quadrupole interaction to be absent in our case. Therefore the spin Hamiltonian including fine-structure splitting is

$$\begin{aligned} HR = {} & H_0 - \tfrac{1}{2}DR(2M-R)(3\cos^2\theta - 1) + (D^2R/8H_0)[4S(S+1) \\ & -24M(M-R) - (8R^2+1)]\sin^2 2\theta - (D^2R/8H_0)[2S(S+1) \\ & - 6M(M-R) - (2R^2+1)]\sin^4\theta - A[r(M-R) + m_I R] \\ & - (A^2/2H_0)[I(I+1)R - Mr(2m_I - r) - m_I R(m_I - 2r) \\ & - r^2 R] + (A^2/2H_0)[S(S+1)R - m_I R(2M-R) - Mr(M \\ & - 2R) - R^2 r]. \end{aligned} \tag{4}$$

Here the constants are to be given in oersteds.

In the derivation of (4) the selection rules for the quantum numbers of shell electron spin and nuclear spin were $\Delta M = R$, $\Delta m_I = r$, where R = 1, 2, 3, 4, 5 and r = 0, ±1, ±2, ±3, ±4, ±5. ($S = \frac{5}{2}$, $I = \frac{5}{2}$).

We have observed forbidden nuclear transitions only in the cases of fine-structure transitions that obeyed the selection rule $\Delta M = 1$. We observed lines with $\Delta m_I = \pm 1, \pm 2$ in the $\frac{1}{2} \rightarrow -\frac{1}{2}$ transition. The positions of these lines relative to the allowed spectrum with $\Delta m_I = 0$ (Fig. 3) yielded the energy level scheme; this in turn gave us the positions of lines with $\Delta m_I = \pm 3, \pm 4, \pm 5$ in the field H, relative to the same allowed transitions. This pattern is shown in Fig. 3. Here the arrows in the upper part denote transitions induced by a quantum $h\nu$; the lower part shows the locations of all forbidden lines (observed or unobserved) in a field H and the allowed hyperfine lines ($\Delta m_I = 0$). It should be noted that the forbidden transitions with $\Delta m_I = \pm 3$ ($\frac{1}{2} \rightarrow -\frac{1}{2}$ transition) which were observed in[2] coincide with our transitions in a

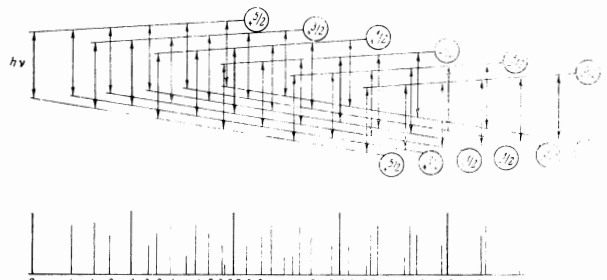

FIG. 3. (Lower part) Allowed ($\Delta m_I = 0$) and forbidden ($\Delta m_I = \pm 1, \pm 2, \pm 3, \pm 4, \pm 5$) spectra of the fine-structure transition 1/2 → −1/2. (Upper part) Hyperfine splitting of the fine-structure levels 1/2 and −1/2 involved in the allowed and forbidden spectra. For the sake of clarity Figs. 3-5 have not been plotted on a common scale, which would show the relative magnitudes of the hyperfine splittings. When Figs. 3-5 are plotted on a single scale the aforementioned quantitative relation between the hyperfine splittings is fulfilled very accurately.

magnetic field.

For the $\frac{3}{2} \rightarrow \frac{1}{2}$ fine-structure transition we observed forbidden transitions with $\Delta m_I = \pm 1, \pm 2$ (Fig. 4). The positions of the forbidden transitions with $\Delta m_I = \pm 1, \pm 2, \pm 3, \pm 4, \pm 5$ in the $\frac{3}{2} \rightarrow \frac{1}{2}$ fine-structure transition exhibit some qualitative departure from the positions of the same lines in the $\frac{1}{2} \rightarrow -\frac{1}{2}$ fine-structure transition. This discrepancy is accounted for by the behavior of the energy levels in the magnetic field.

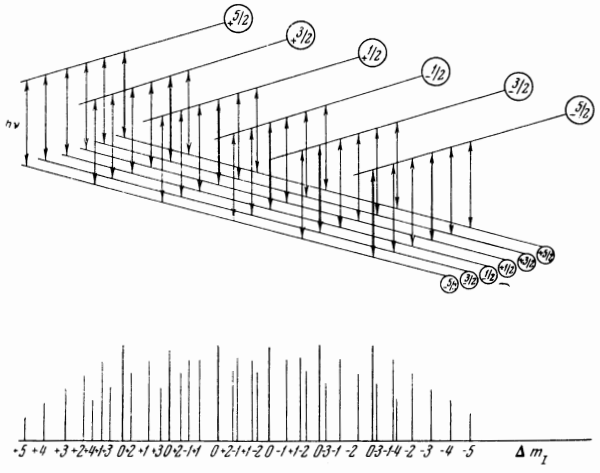

FIG. 4. (Lower part) Allowed ($\Delta m_I = 0$) and forbidden ($\Delta m_I = \pm 1, \pm 2, \pm 3, \pm 4, \pm 5$) spectra of the fine-structure transition $3/2 \rightarrow 1/2$. (Upper part) Hyperfine splitting of the fine-structure levels 3/2 and 1/2. The forbidden spectrum of the $-1/2 \rightarrow -3/2$ fine-structure transition is completely similar. The easily constructed hyperfine structures of the $-1/2$ and $-3/2$ levels are exactly like those of the 3/2 and 1/2 levels.

Forbidden transitions with $\Delta m_I = \pm 1$ were also observed for the $\frac{5}{2} \rightarrow \frac{3}{2}$ fine-structure transition, and are shown in Fig. 5 along with all the other transitions ($\Delta m_I = \pm 2, \pm 3, \pm 4, \pm 5$). Because of the particular hyperfine splittings we find that the forbidden lines are shifted somewhat from the forbidden lines of the $\frac{3}{2} \rightarrow \frac{1}{2}$ and $\frac{1}{2} \rightarrow -\frac{1}{2}$ transitions.

In constructing Figs. 3–5 we did not use a consistent scale for the transition-inducing quanta or for the relation between these quanta and the separations of the experimentally observed lines. Nevertheless, these figures present a picture that is qualitatively correct. We note, for example, that the hyperfine splitting of the $\frac{5}{2}$ fine-structure level is five times greater than the hyperfine splitting of the $\frac{1}{2}$ level and that the splitting of the $\frac{3}{2}$ level is three times greater than that of the $\frac{1}{2}$ level (using arbitrary units for the splittings). This pattern is easily accounted for in virtue of the fact that the magnetic moments of the $\frac{5}{2}$ and $\frac{3}{2}$ states are 5 and 3 times greater, respectively, than that of the $\frac{1}{2}$ state. We thus arrive easily at the conclusion that the hyperfine splitting is accounted for entirely and exclusively by the interaction between the dipole moments of shell electrons and the dipole moment of the nucleus (the dipole-dipole interaction). If at the same time an interaction should exist between the electric field of the electrons and the nuclear quadrupole moment (the quadrupole interaction) we would not find such a simple relationship governing the hyperfine

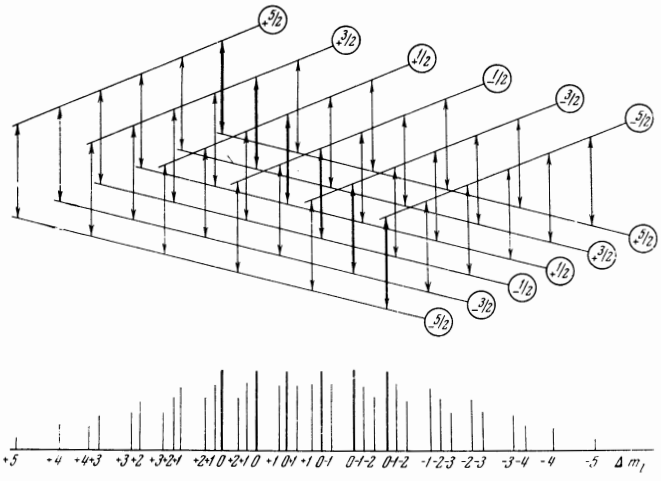

FIG. 5. Allowed ($\Delta m_I = 0$) and forbidden ($\Delta m_I = \pm 1, \pm 2, \pm 3, \pm 4, \pm 5$) spectra of the $5/2 \rightarrow 3/2$ fine-structure transition. Upper part – energy levels; lower part – lines in a magnetic field H.

splitting. We must therefore assume either zero quadrupole moment of the Mn nucleus or that the quadrupole interaction constant Q [in Eq. (3)] is smaller than the experimental error (~0.5 Oe). The absence of a quadrupole interaction is indicated by the fact that the hyperfine line separation remains constant as the angle θ is varied (Fig. 2). This would not occur if Q did not vanish; the hyperfine line separation would then obey a $(3\cos^2\theta - 1)$ law.

We note, in conclusion, that all our spectra (allowed and forbidden, observed and unobserved) are in good agreement with Eq. (4).

[1] F. K. Hurd, M. Sachs, and W. D. Hershberger, Phys. Rev. **93**, 373 (1954).

[2] C. Kikuchi and L. M. Matarrese, J. Chem. Phys. **33**, 601 (1960).

[3] L. M. Matarrese, J. Chem. Phys. **34**, 336 (1961).

[4] B. Bleaney and R. S. Rubins, Proc. Phys. Soc. (London) **77**, 103 (1961).

[5] A. Nucula, Rev. roumaine phys. **10**, No. 2 (1965).

[6] J. Ursu, Rev. roumaine phys. **11**, No. 9 (1966).

[7] E. Lambert and F. Porret, Helv. phys. acta **39**, 585 (1966).

[8] V. N. Lazukin and A. N. Terent'evskiĭ, Vestnik Moscow State Univ., ser. fiz.-astron. **6**, 105 (1967).

[9] W. Low, Phys. Rev. **105**, 801 (1957).

[10] H. Watanabe, Progr. Theoret. Phys. (Kyoto) **18**, 405 (1957).

[11] R. S. Title, Phys. Rev. **131**, 623 (1963).

[12] W. H. From, P. B. Dorain, and C. Kikuchi, Phys. Rev. **135**, A710 (1964).

[13] R. N. Hall, Phys. Rev. **87**, 387 (1952).

[14] H. B. Nudelman, Phys. Chem. Solids **26**, No. 6 (1965).

[15] H. Strunz, Mineralogical Tables, Gosgortekhizdat, 1962.

[16] G. L. Bir and I. V. Vinokurov, Fiz. Tverd. Tela **7**, 3392 (1965) [Sov. Phys.-Solid State **7**, 2730 (1966)].

Translated by I. Emin
179